Available online at www.sciencedirect.com
SCIENCE DIRECT
Journal of Power Sources 157 (2006) 358–367
JOURNAL OF POWER SOURCES
www.elsevier.com/locate/jpowsour

Pressure drop and flow distribution in multiple parallel-channel configurations used in proton-exchange membrane fuel cell stacks

S. Maharudrayya, S. Jayanti *, A.P. Deshpande

Department of Chemical Engineering, IIT-Madras, Chennai 600036, Tamil Nadu, India

Received 6 May 2005; accepted 25 July 2005
Available online 12 September 2005

Abstract

Single U- and Z-type parallel-channel configurations for gas distributor plates in planar fuel cells reduce the pressure drop but give rise to the problem of severe flow maldistribution wherein some of the channels may be starved of the reactants. In this paper, previous analytical solutions obtained for single U- and Z-type flow configurations are extended to multiple U- and multiple Z-type flow configurations of interest to fuel cell applications. Algorithms to calculate flow distribution and pressure drop in multiple U- and Z-type flow configurations are developed. The results are validated by comparison with those obtained from three-dimensional computational fluid dynamics (CFD) simulations. It is found that there is a significant improvement in the flow distribution in some configurations without paying for extra pressure drop. The possibility of unmatched distribution on the cathode and the anodes sides is also highlighted. Careful design of the flow configuration is therefore necessary for optimum performance.

Keywords: Parallel channels; Laminar flow; Flow distribution; Pressure drop; Computational fluid dynamics; Proton-exchange membrane fuel cell

1. Introduction

A planar architecture for the gas distribution channels of proton-exchange membrane fuel cells (PEMFCs) provides an effective approach and achieves high utilization of the electrochemically active area. Many designs of flow configurations, for example, serpentine, parallel, parallel serpentine, discontinuous, conventional and interdigitated channel (Fig. 1), are currently in use to distribute the reactants [1–5]. There are principally two considerations in the choice of a particular configuration: (i) the overall pressure drop and (ii) the degree of non-uniformity of flow distribution over the plate. Single serpentine channels have guaranteed uniformity of flow over the entire channel but may have excessive pressure drop. It has been estimated [4] that the pressure drop required for a serpentine channel may be an order of magnitude higher than that required for a parallel channel. By comparison, simple parallel channels, such as the single-U type and the single-Z type (Fig. 1(b) and (c), respectively) may suffer from severe flow maldistribution problems. The severity of this problem for PEMFCs has been demonstrated theoretically by Kee et al. [2] and the present authors [1], and has also been examined experimentally by Barreras et al. [6]. More complicated configurations may show even more complicated behaviour. A case in point is the conventional or double-U type of configuration (Fig. 1(f)), which has often used by researchers. The flow distribution in this can be very sensitive to the location of the central rib relative to the flow inlet. This is demonstrated in Fig. 2 where the relative flow distribution in a 21-channel is calculated using the computational fluid dynamics (CFD) techniques described previously [1]. The flow distribution corresponding to the conventional configuration, where there is no rib in front of the inlet channel, is shown in Fig. 2(a). Here, there is a large bypass of the flow through the central channel and this causes severe non-uniformity of flow. When the design is slightly changed by placing a central rib (Fig. 2(b)), the flow distribution becomes much less distorted (Fig. 2(c)) although it is still by no means uniform.

* Corresponding author. Tel.: +91 44 22574168; fax: +91 44 22570509.
E-mail address: sjayanti@iitm.ac.in (S. Jayanti).

0378-7753/$ – see front matter © 2005 Elsevier B.V. All rights reserved.
doi:10.1016/j.jpowsour.2005.07.064

Nomenclature

a	aspect ratio (width/depth)
A_c	cross-sectional area of channel (m^2)
A_h	cross-sectional area of header (m^2)
b_c	depth of channel (m)
b_h	depth of header (m)
C	curvature ratio
C_1	constant
C_2	constant
C_3	constant
C_4	constant
D_c	hydraulic-diameter of channel (m)
D_h	hydraulic-diameter of header (m)
F_1	flow non-uniformity index
f	friction factor
i	channel number
K_1	flow distribution parameter
K_2	flow distribution parameter
K_{fric}	frictional loss factor
L_c	length of the channel m
L_h	length of the header m
m	constant
m'_c	relative mass flow rate
N	number of channels
n	constant
P	pressure
P_h	perimeter of the header, m
Re	Reynolds number
V_c	velocity in the channel header (m^{-1} s)
w	width (m)
x	cartesian coordinate

Greek letters

Δ	difference operator
μ	absolute viscosity (kg m^{-1} s^{-1})
ρ	density (kg m^{-3})
τ_w	wall shear stress (N m^{-2})
ξ	excess bend loss coefficient

Superscripts

c	channel
in	inlet
h	header
max	maximum
min	minimum
r	rib
s	spacer length
U	U-type
$'$	all prime values are dimensionless variables

The consequences of flow maldistribution in channels may be severe. Some channels may be starved of the reactants, while others may have them in excess. Since the reactant distribution manifolds on the anode and the cathode sides are hydrodynamically de-coupled, severe maldistribution of the reactants is possible across the membrane–electrode assembly (MEA). Often, the relative flow distribution in a parallel channel is a function of the flow rate. Since the volumetric flow rates on the anode and the cathode sides differ by a large amount, there may not be good matching of the relative flow distribution and correct stoichiometry may not be ensured unless the distributor plates are properly designed.

The problem of flow distribution in fuel cell channels has received rigorous treatment in recent years. Kee et al. [2] first raised the possibility of maldistribution and presented a numerical model to calculate the flow distribution in a Z-type parallel configuration. Work in our laboratories has extended [1] the analysis to U-type parallel configurations and has obtained closed form analytical solutions to calculate the flow distribution and the pressure drop in simple parallel channels. The models show that severe maldistribution is possible under typical geometric and flow conditions of PEMFC distributor plates. Recently, Barreras et al. [6] provided experimental evidence of flow maldistribution in a 16-channel Z-type configuration on a distributor plate of 50 cm^2 for the flow of water and glycerin at Reynolds numbers in the range of 60–150. They also reported good agreement between their experiments and CFD computations.

Against this background, the purpose of the present work is to extend the previously reported hydrodynamic analysis of simple U- and Z-type configurations [1] to multiple U- and Z-type configurations of the type shown in Figs. 1(e) and 2(b). To this end, a formal analytical treatment of 2U-, 4U- and 5Z-parallel-channel configurations has been performed to obtain the relative flow distribution and overall pressure drop using an algorithmic approach. The overall results of the models are compared with full three-dimensional CFD calculations using a commercial software. It is found that a much better flow distribution, at relatively little increase in pressure drop, can be obtained with certain types of multiple-parallel configurations.

2. Problem formulation

2.1. Overview

From a hydrodynamic point of view, the various channel configurations illustrated in Fig. 1 can be seen to be combinations of the flows in the straight channels of a rectangular cross-section of given aspect ratio. Typical channel dimensions and flow rates used in PEMFCs are such that the flow is invariably laminar and the Reynolds number is typically less than about 300 in the individual parallel channels. Under these conditions, design correlations for the calculation of the pressure drop and flow distribution are available from earlier systematic studies [1,4]. These enable the calculation of the following:

- the frictional pressure gradient in a fully-developed flow in a duct of rectangular cross-section of given aspect ratio;

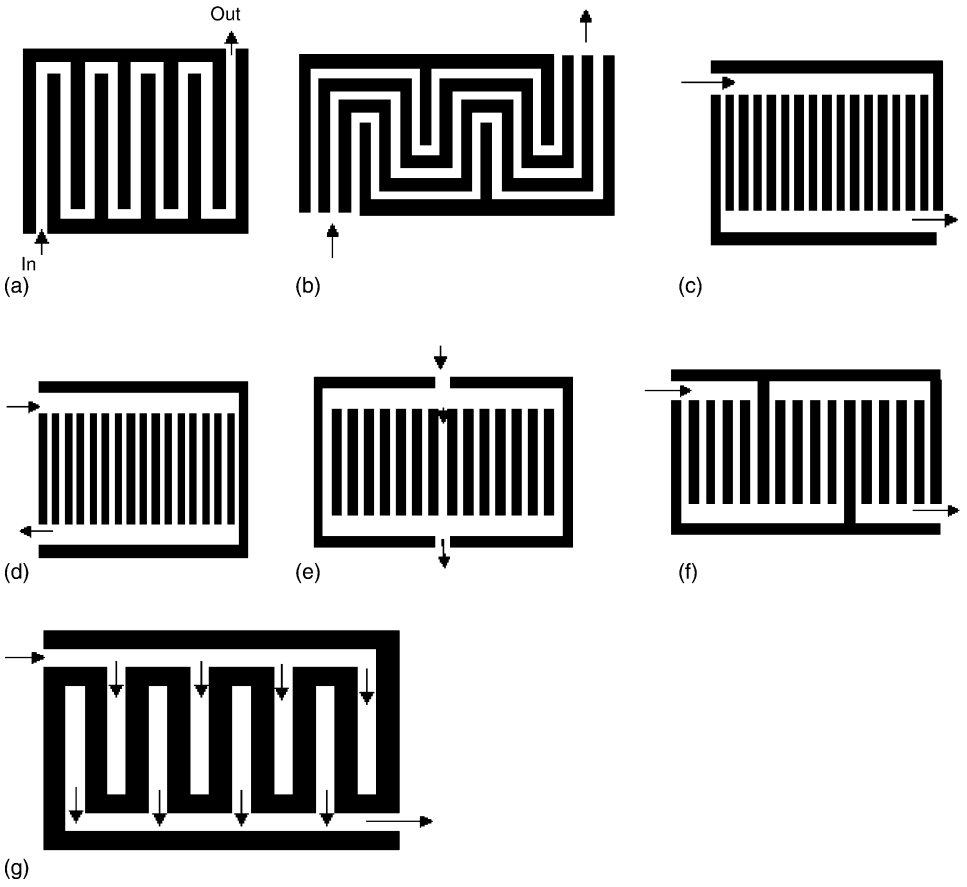

Fig. 1. Schematic diagram of (a) single serpentine; (b) parallel serpentine; (c) single Z-type; (d) single Z-type; (e) conventional type; (f) discontinuous type; (g) interdigitated type channel configurations.

- the pressure loss at a bend of arbitrary curvature ratio;
- the flow distribution in a parallel channel of a single U-type (Fig. 1(b)) or a single Z-type (Fig. 1(c)) with an arbitrary number of identical parallel channels;
- the pressure drop between the inlet and the outlet for the U- and the Z-type configurations for a given overall volumetric flow rate.

In the present study, these basic serpentine- and parallel-channel elements are put together to extend the analysis to three other configurations, namely: (i) the conventional type (Fig. 3(a)), which can be seen as a combination of two U-type flow channels; (ii) the multiple-U type (Fig. 3(b)), in which one conventional type is embedded in another; (iii) the discontinuous type (Fig. 1(f)), which is a combination of several Z-type parallel channels connected in series. Algorithms have been developed to calculate the flow distribution in each of these three channels as well as the overall pressure drop between the inlet and the outlet for each configuration. Details of the models are described below.

2.2. Flow in simple configurations

For the sake of completeness, the results obtained previously [1,4] for single serpentine and U- and Z-type channels are reproduced here for later use.

2.2.1. Single serpentine channels

In the analysis of multiple-parallel channels, the bend losses are neglected as the Reynolds numbers are typically less than 300. Under such conditions, the excess bend pressure loss coefficient is negligible. The total pressure drop in a straight duct can be calculated as

$$\Delta P_{\text{tot}} = \frac{1}{2}\rho V^2 \left(\frac{4fL}{D_{\text{h}}} + \sum_{i=1}^{n} \xi_i \right) \tag{1}$$

where the friction factor f is given by the relation of Kays and Crawford [7] and ξ_i is the excess bend loss coefficient of the ith bend, which is given by [4]

For $Re < 100$

$$\xi = 0 \tag{2a}$$

For $100 < Re < 1000$

$$\xi = 0.46(Re^{1/3})(1 - 0.18C + 0.016C^2) \times (1 - 0.2a + 0.0022a^2) \times \left(1 + 0.26\left(\frac{L_{\text{s}}}{D_{\text{h}}}\right)^{2/3} - 0.0018\left(\frac{L_{\text{s}}}{D_{\text{h}}}\right)^{2} \right) \tag{2b}$$

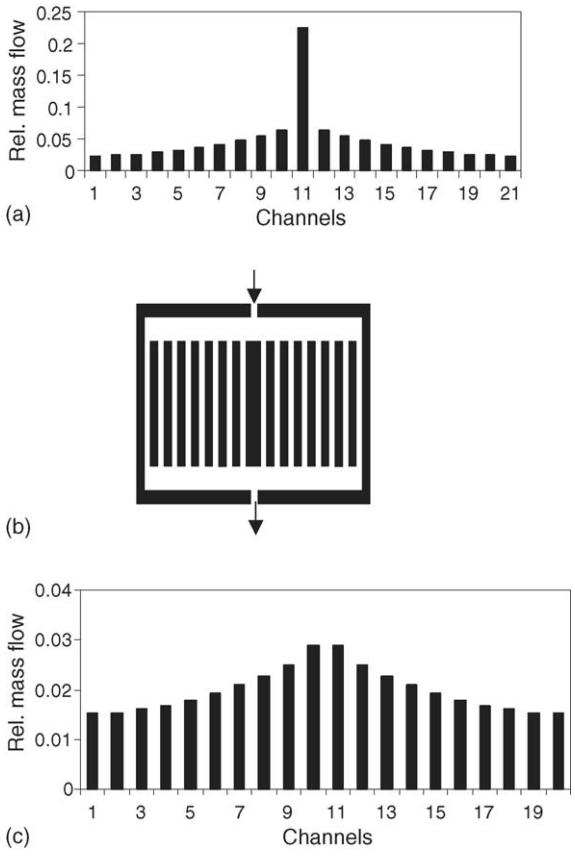

Fig. 2. (a) Relative flow distribution in conventional-type flow configuration obtained from CFD calculations; (b) schematic diagram of modified conventional (2U)-type flow configuration; (c) relative flow distribution obtained from CFD simulations for modified conventional-type channel.

For $1000 < Re < 2200$

$$\xi = 3.8(1 - 0.22C + 0.022C^2)(1 - 0.1a + 0.0063a^2) \times \left(1 + 0.12\left(\frac{L_s}{D_h}\right)^{2/3} - 0.0003\left(\frac{L_s}{D_h}\right)^2\right) \quad (2c)$$

$$Ref = 13.84 + 10.38\ \exp\left(\frac{-3.4}{a}\right) \quad (2d)$$

where a is the channel aspect ratio ($a = w/b$); C, the bend curvature ratio; L_s, the distance between two consecutive bends.

2.2.2. Single Z-type channel

This flow is characterized [1] by two dimensionless parameters K_1 and K_2 defined as:

$$K_1 = \left(\frac{NA_c\rho V_{in}}{A_h}\right)\frac{D_c^2}{(Ref)_c 2L_c\mu} \quad (3a)$$

$$K_2 = \left(\frac{P_h\mu(Ref)_h L_h}{2A_h D_h\rho V_{in}}\right) \quad (3b)$$

where N is the number of parallel channels; A_c and A_h, the cross-sectional areas of the channel and the header, respectively, and D_c and D_h are their respective hydraulic diameters; L_c and L_h, the respective lengths; V_{in}, the header inlet velocity; P_h, the header perimeter; ρ and μ, the density and the dynamic viscosity of the fluid, respectively; (Ref) is the product of the friction factor and the Reynolds number given by Eq. (2) above.

The overall pressure drop between the inlet and the outlet in this case is given [1] by:

$$\Delta P = \Big\{C_1^2(\exp(2m) - 1) + C_2^2(\exp(2n) - 1) + \frac{K_1C_1 + C_1m}{m}(\exp(m) - 1) + \frac{K_2C_2 + C_2n}{n}(\exp(n) - 1) + 0.5K_2 - \frac{C_1\exp(m) + C_2\exp(n)}{K_1} + 4C_1C_2(\exp((m + n)) - 1)\Big\}\rho V_{in}^2 \quad (4)$$

Here m and n are given in terms of K_1 and K_2 as:

$$m = K_1 + \sqrt{K_1^2 + 2K_1K_2}, \quad n = K_1 - \sqrt{K_1^2 + 2K_1K_2} \quad (5a)$$

and C_1 and C_2 are expressed as:

$$C_1 = \frac{0.5(1 + \exp(n))}{(\exp(n) - \exp(m))}, \quad C_2 = \frac{0.5(1 + \exp(m))}{(\exp(m) - \exp(n))} \quad (5b)$$

The relative flow rate distribution in the ith channel is given by the following expression:

$$m'_{ci} = -\frac{(C_1m\ \exp(mx'_i) + C_2n\ \exp(nx'_i))}{N} \quad (6)$$

where $x'_i = x_i/L_h$ is the non-dimensional distance of the channel from the inlet header.

2.2.3. Single U-type channels

The pressure drop between the inlet and the outlet of the manifold is given by the following relation

$$\Delta P = -\frac{(C_3m' + C_4n')\rho V_{in}^2}{K_1} \quad (7)$$

where $m' = -n' = \sqrt{2K_1K_2}$ and C_3 and C_4 are expressed by:

$$C_3 = \frac{-\exp(n')}{(\exp(m') - \exp(n'))}, \quad C_4 = \frac{\exp(m')}{(\exp(m') - \exp(n'))} \quad (8a\text{-}b)$$

The relative flow rate distribution is given by:

$$m'_{ci} = -\frac{(C_3m'\ \exp(m'x'_i) + C_4n'\ \exp(n'x'_i))}{N} \quad (9)$$

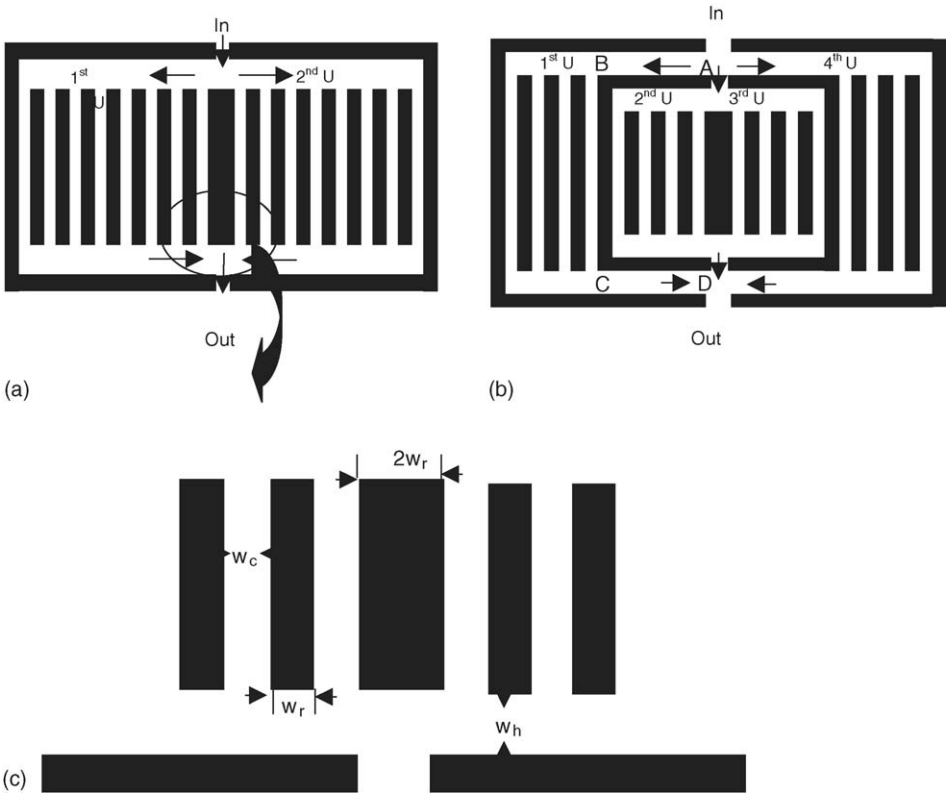

Fig. 3. Schematic diagram showing combinations of U-type configurations in (a) 2U-type (b) 4U-type; (c) enlarged view near main flow inlet and dimensions in 2U-type configuration.

where x_i' is the non-dimensional distance from the inlet header for the ith channel.

2.3. Analysis of conventional-type configuration

In this configuration (Fig. 1(e)), the flow distribution is expected to be symmetrical about the vertical centre-line. The geometry considered here is somewhat different from the purely conventional type; a central rib of twice the width of the other ribs is placed directly opposite the inlet (Fig. 2(b)) to minimize the bypassing that may otherwise take place (Fig. 2(a)). With this arrangement, the flow in each half-section is given by the equations corresponding to the single U-configuration (i.e., Eq. (7) for pressure drop and Eq. (9) for relative mass flow rate) with the modification that N corresponds to the number of channels in each half-section. The total pressure drop in the manifold is equal to the sum of the pressure drop due to the U-type parallel channels and the pressure drop due to the flow turn by the 90° bend at the main inlet and exit sections.

2.4. Analysis of 4-U configuration

This configuration has four single U-type configurations: two (first and second U) to the left side of the vertical symmetry line and two (third and fourth U) to the right side (Fig. 3(b) and (c)). Because of symmetry, it is expected that the flow distribution in the first U will be the same as that in the third U, and that the flow distribution in the second U will be the same as that in the fourth U. Though the main flow divides equally into the left and right sides, the first and the second U need not have the same flow rate. When compared with the parallel channels in the second U, those in the first U are slightly longer and the flow has to traverse the length of the header of the second U before it enters the first U. Both factors decrease the pressure head available for flow in the first U and lead to a lower flow rate. If $V_{h,1U}$ is the mean flow velocity in the header of the first U, then the pressure drops across the two U, with reference to Fig. 2(b), are related as follows:

$$\Delta P_{AD} = \Delta P_{BC} + \frac{8L_{AB}f}{D_{h,1U}}\frac{1}{2}\rho V_{h,1U}^2 \tag{10}$$

where L_{AB} is the extra length that the fluid has to travel in order to reach the first U. Now, ΔP_{AB} and ΔP_{CD} can be related to the flow rates and geometric parameters of the second and the first U, respectively, by Eq. (7) above, which can be rewritten as:

$$\Delta P_{BC} = b_{1U} Q_{h,1U} \tag{11}$$

where $Q_{h,1U}$ is the volumetric flow rate through the header of the first U and b_{1U} is given by:

$$b_{1U} = \left(-\frac{2(C_3 m' + C_4 n')(Ref)_c L_c \mu}{N A_c D_c^2} \right)_{1U} \quad (12)$$

Thus, Eq. (10) can be written as:

$$b_{2U} Q_{h,2U} = \left(b_{1U} + \frac{2(Ref)_h L_{h1} \mu}{D_{h,1U}^2 A_h} \right)_{1U} Q_{h,1U} \quad (13)$$

Noting also that

$$Q_{h,1U} + Q_{h,2U} = \frac{Q_{total}}{2} \quad (14)$$

the following expressions for the flow through each U can be obtained as follows:

$$Q_{h,1U} = \frac{Q_{total} b_{2U}}{2(b_{1U} + b_{2U})} \quad (15a)$$

$$Q_{h,2U} = \frac{Q_{total} b_{1U}}{2 b_{2U}} \quad (15b)$$

where

$$b_{1U} = \left(-\frac{2(C_3 m' + C_4 n')(Ref)_c L_c \mu}{N A_c D_c^2} \right)_{1U} \quad (16a)$$

$$b_{2U} = \left(-\frac{2(C_3 m' + C_4 n')(Ref)_c L_c \mu}{N A_c D_c^2} \right)_{2U} \quad (16b)$$

The overall pressure drop across the plate can be taken to be equal to ΔP_{AD} and is given by

$$\Delta P_{AD} = b_{2U} Q_{h,2U} \quad (17)$$

With these results, the following algorithm can be used to obtain the flow distribution and the pressure drop in the 4U-type configuration:

Step I: compute b_{1U} and b_{2U} using Eqs. (16a) and (16b).
Step II: compute flow rate through the first and the second U using Eqs. (15a) and (15b).
Step III: compute the relative flow distribution in each channel of the first U and second U by using Eq. (9) and the appropriate channel header velocity and channel dimensions to calculate K_1 and K_2 from Eqs. (3a) and (3b).
Step IV: obtain the flow rate in each channel by multiplying the relative channel distribution with the total flow rate through the respective U.
Step V: calculate the pressure drop across the plate using Eq. (17).

2.5. Analysis of discontinuous channel

This configuration (Fig. 1(f)) can be viewed as a number of Z-type channels connected in series. Therefore, the flow rate through each Z will be the same and will be equal to the total flow rate through the plate. If each Z is identical to the other, the relative flow rate distribution in each will be identical and is given by Eq. (6); if not, for example, if one Z has more parallel channels, then the relative flow rate distribution can still be obtained from Eq. (6) using the appropriate channel values. The overall pressure drop is obtained by summing the pressure drop across each Z. Thus, the following algorithm can be used to obtain the flow distribution and the pressure drop in the discontinuous type configuration:

Step I: use Eq. (6) with appropriate channel and header dimensions to calculate the relative flow rate distribution in each Z.
Step II: use Eq. (4) to calculate the pressure drop across each Z with the appropriate channel dimensions.
Step III: add the pressure drop across each individual Z channel to obtain the overall pressure drop.

3. Validation

The accuracy of the above algorithms has been verified by comparing the analytical results with those obtained from CFD simulations carried out for specific cases as part of the present study. Details of the CFD simulations are similar to those that have already been employed by the present authors [1] for the validation of the single U and the single Z configurations. For validation of the multiple U- and Z-configurations, laminar flow through 20 parallel channels in a 2U-, 4U-type or multiple Z-type configuration has been calculated using the commercial CFD code *CFX* developed by AEA Technology, UK. The simulations cover a range of flow rates for fixed values (typical of PEMFC gas distributor plates) of the geometric parameters. Comparison between the analytical and the CFD results of the relative distribution of the mass flow rates is shown in Fig. 4 for the three configurations at an inlet mass flow rate of 1.44^{-5} kg s^{-1}. There is a good agreement between the analytical and the CFD solutions. The predicted pressure drops are compared in Fig. 5(a) and (b) for the 2U and the 5-Z configurations, respectively. There is a good agreement between the two sets of data. Given that no approximations are made in the momentum balance equations in the CFD solution, this good agreement demonstrates that accurate predictions of the distributions of flow rate and pressure drop in multiple U and Z configurations can be obtained by means of the relations proposed above.

4. Results and discussion

4.1. Analysis of multiple U-type configurations

In previous studies [1,2], the relative flow distribution in parallel channels has been characterized using a flow non-uniformity index (F_1) defined as:

$$F_1 = \frac{(m'_{c,max} - m'_{c,min})}{m'_{c,max}} \quad (18)$$

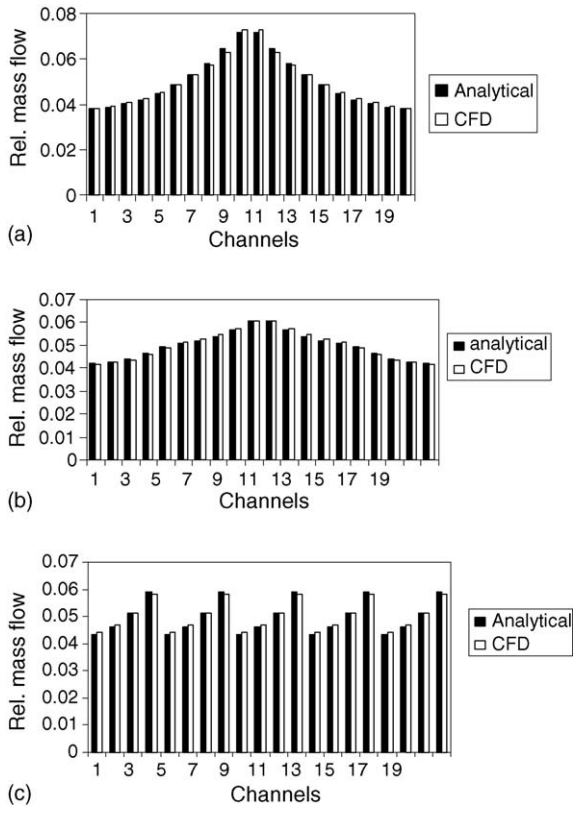

Fig. 4. Validation of analytical results by CFD simulations for (a) 2U-type; (b) 4U-type; (c) discontinuous channel configurations.

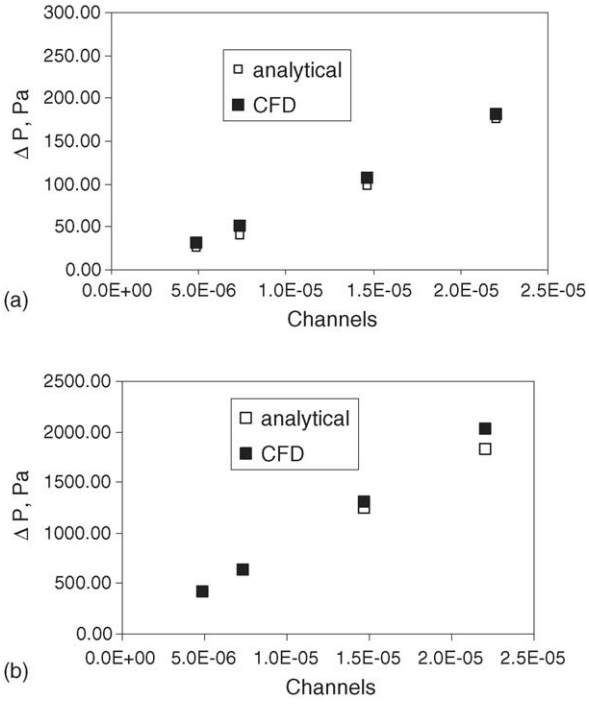

Fig. 5. Comparison of pressure drop obtained from analytical and CFD-solution in (a) 2U-type; (b) 5-Z type channel configuration.

Here, $m'_{c,max}$ and $m'_{c,mix}$ are the maximum and minimum flow rates in a set of parallel channels. The value of F_1 varies between 0 and 1 and indicates the extent of non-uniformity of flow distribution among channels. If $F_1 = 0$, then all the channels have the same flow rate. If $F_1 = 1$, then at least one channel has zero flow rate and the flow distribution is therefore highly skewed. It has been found [1] that the value of the flow distribution index in a single U-type flow configuration depends on the values of the resistance parameters K_1 and K_2. All other things being equal, the lower the value of K_1, the better, i.e., the more uniform, is the flow distribution. For a given cell active area and the overall flow rates of the reactants, it is possible to reduce K_1 by using multiple-U configurations. This has the effect of decreasing the number of parallel channels in each U and therefore decreases K_1. This is shown in Fig. 6 where calculations of the flow distribution have been presented for a set of 40 channels arranged in a single-U, a 2-U or a 4-U configuration. In all the three cases, the air inlet mass flow rate is kept constant at 2.2×10^{-5} kg s^{-1} and the geometric parameters are kept constant at a header width of 4 mm and depth of 1.5 mm, a channel width of 2 mm and depth of 0.72 mm, and a rib width of 2 mm There is severe flow maldistribution in the case of the single-U, configuration with a flow distribution index value of 0.70. The situation is improved with a 2-U configuration and the flow non-uniformity index comes down to 0.30. A nearly uniform flow rate, with a flow non-uniformity index of 0.16 is obtained with a 4-U configuration. The pressure drop corresponding to these cases is given in Table 1. It is seen that a significant improvement in the flow distribution index is achieved by a relatively small increase of about 20% in the overall plate pressure drop. Thus, a 4-U configuration is clearly superior to that of a single-U.

Table 1
Comparison of flow distribution parameters and index and pressure for different U-type and Z-type flow configurations

Mass flow rate (kg s^{-1})	Configurations	K_1	K_2	Flow non-uniformity index (F_1)	ΔP (Pa)
2.2E-05	1-U	3.41E−01	5.48	0.70	66.75
	2-U	8.51E−02	5.48	0.30	76.51
	4-U	2.26E−02	5.27	0.16	78.22
2.2E-05	1-Z	3.41E−01	5.48	0.48	73.75
	2-Z	1.70E−01	2.74	0.27	170.79
	4-Z	8.51E−02	1.37	0.15	554.62
	5-Z	6.81E−02	1.10	0.12	842.71

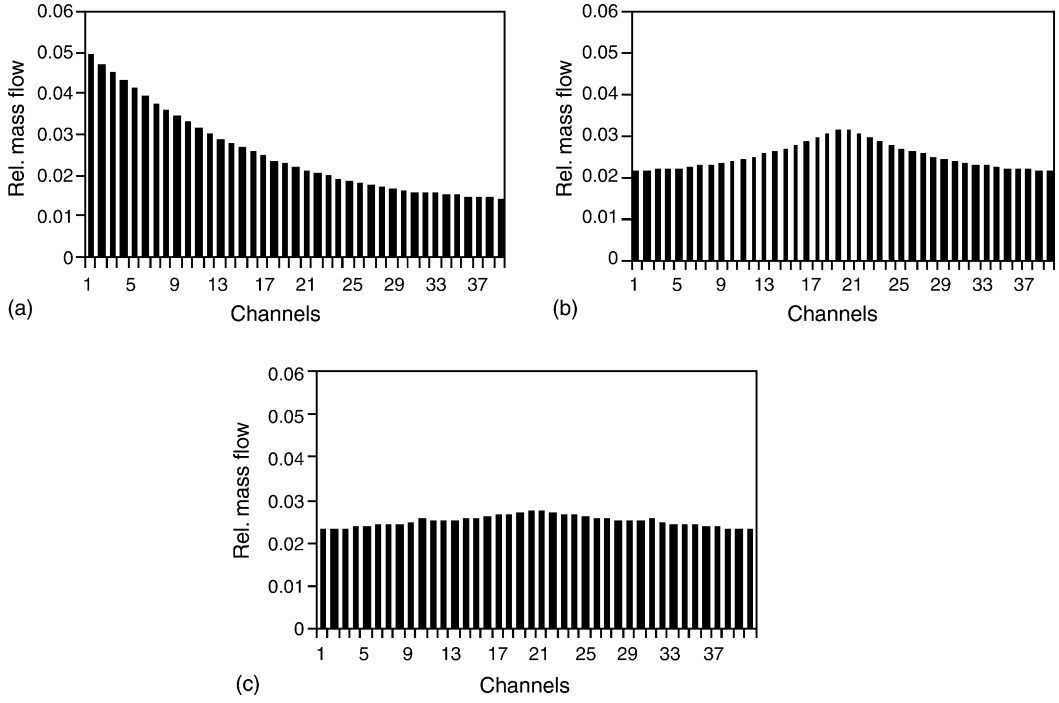

Fig. 6. Flow distributions in (a) single U-type; (b) 2U-type and (c) 4U-type flow configurations.

4.2. Analysis of multiple Z-type flow configurations

The situation in multiple Z-type configurations is similar in some respects to that in multiple U-type configurations. The flow distribution index can be improved by increasing the number of single-Z configurations in series. In the literature, such channels are known as the discontinuous channels and have been reported [8–12] to perform very well compared with a single Z-type flow configuration in terms of fuel cell efficiency. This may be attributed to the severe flow maldistribution in single-Z flow configurations compared with multiple Z-type configurations, and is illustrated in Fig. 7 that shows the relative flow distributions for single Z, two-Z, four-Z and five-Z configurations. The channel

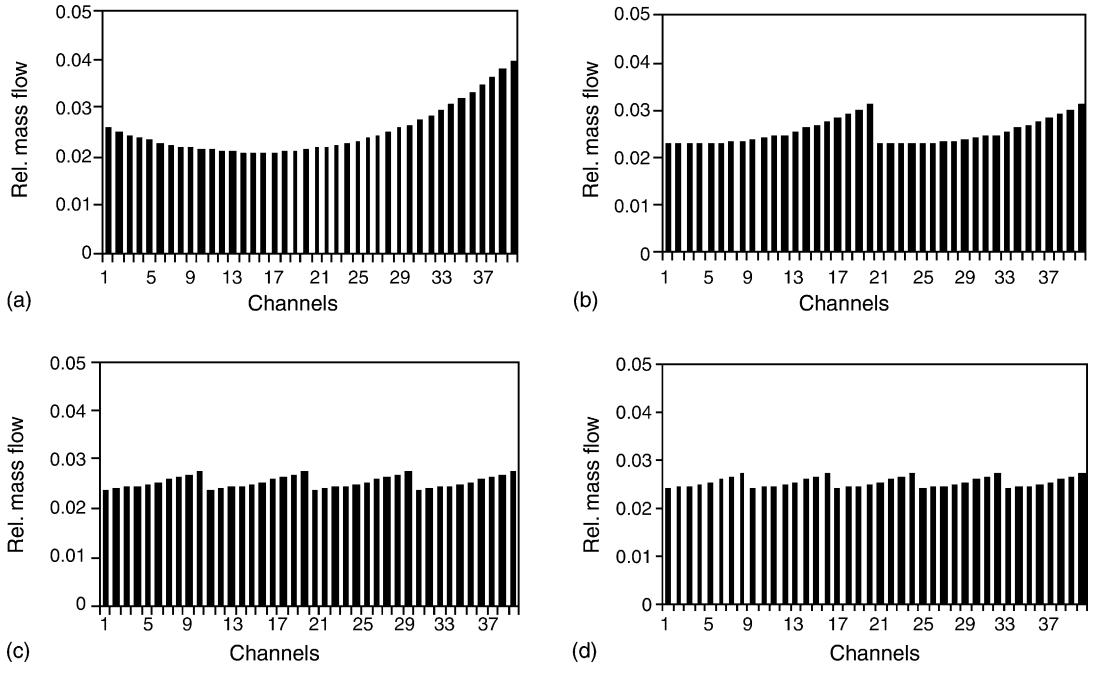

Fig. 7. Flow distributions in (a) single Z-type; (b) 2-Z; (c) 4-Z; (d) 5-Z configuration obtained from present model.

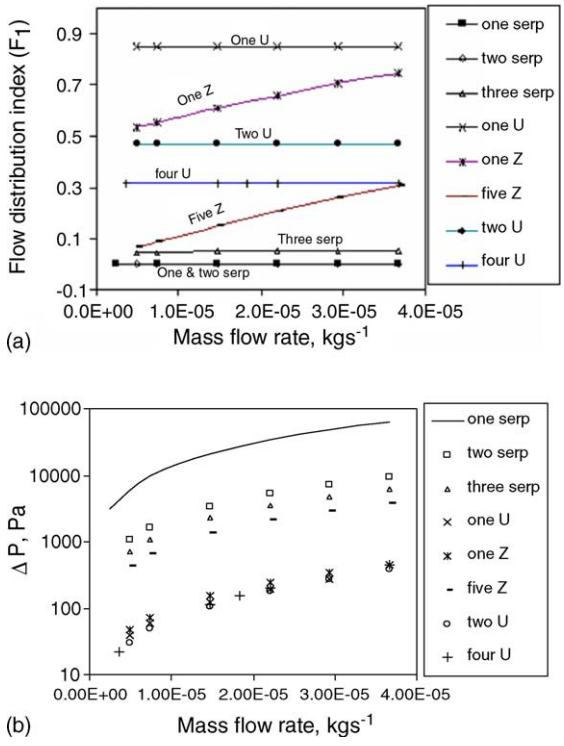

Fig. 8. Variation of (a) flow non-uniformity index; (b) pressure drop with inlet mass flow rate for various flow configurations.

dimensions, the overall flow rate, the cell active area and the mass flow rate in these three versions are the same as those in the multiple-U configurations shown in Fig. 5. The single-Z configuration has a non-uniform flow distribution with a flow non-uniformity index of 0.48. This reduces to 0.25 with a two-Z configuration and to 0.15 and 0.12 with a 4-Z and 5-Z configuration, respectively. The corresponding pressure drops for each case are given in Table 1. The data show that an improvement in flow distribution is obtained at the cost of significant pressure drop, which for a 5-Z configuration is more than 10 times that for a single-Z configuration.

4.3. Comparison of various flow configurations

Since design correlations for all the flow configurations are now available, the relative performance, from a hydrodynamic point of view, of the various channel configurations shown in Fig. 1 can be assessed. To this end, calculations of the flow distribution index and the pressure drop have been made over a range of air flow rates for the same active cell area. The geometric parameters are kept constant at a header width of 4 mm and depth of 1.5 mm, a channel width of 2 mm and depth of 0.72 mm, and a rib width of 2 mm. The calculated plate flow non-uniformity index and the pressure drop for single and parallel serpentine configurations are shown in Fig. 8(a) and (b), respectively, for single, as well as multiple U- and Z-type configurations with 20 channels. All these results have been obtained from the analytical models presented above and show very good agreement with CFD simulations. It can be seen that, as expected, the single serpentine configuration, which has a desirable flow distribution index of zero, has the highest pressure drop. When two or three parallel serpentine channels are used, the pressure drop is reduced with three parallel channels, however, the distribution index becomes positive and thus the flow rate through each channel is not the same. The single-Z and the single- and multiple-U configurations experience a considerably lower pressure drop but also have a relatively high flow non-uniformity index. For a U-type configuration, the flow non-uniformity index is independent of the flow rate (as has been pointed out previously [1]) while for a Z-type configuration, it increases with increasing flow rate. Generally, the higher the number of modules of U- or Z-type, the lower is the flow distribution index and the higher is the pressure drop. Thus, the five-Z configuration that has, over the range of flow rates considered here, the lowest flow distribution among the multiple parallel-channel configurations, also has the highest pressure drop. There is clearly a possibility for optimization on a case-to-case basis.

4.4. The need to optimize

While the possibility for optimization clearly exists, there is also a need to optimize. It has been shown in Fig. 2 that the conventional channel configuration can experience severe problems of non-uniform flow distribution. What is perhaps not readily appreciated is the possibility of unmatched distribution of reactants on either side of the membrane. This is illustrated in Fig. 9(a) where the relative flow distribution is calculated for hydrogen and air in a 22-channel Z-type configuration with identical dimensions on the cathode and the anode sides. The overall flow rate of air is 1500 ml min^{-1} (6.25×10^{-5} kg s^{-1}) while the, overall flow rate of hydrogen is 250 ml min^{-1} (8.3×10^{-7} kg s^{-1}). This gives a stoichiometry ratio of 3.2 for air and 1.6 for hydrogen at a current density of 1 A cm^{-2} for hydrogen at a system pressure of 2 bar. Since the relative flow rate distribution in a Z-type channel is a function of the flow rate, the calculated distributions on the cathode and the anode side do not match and the estimated local stoichiometric ratio can be different, as shown in Fig. 9(b) where the stoichiometric ratios are plotted on a logarithmic scale. For an average current density of 1 A cm^{-2}, many of the channels are starved of reactants on the cathode side as the air flow rate is less than stoichiometry for the given current density. The hydrogen flow rate remains slightly higher than stoichiometry in all cases. Some of the central channels may be starved of hydrogen if the current density is increased. This factor, namely, the discrepancy between the global and the local stoichiometric ratios for the reactants, should be taken into account when designing the channel configurations for distributor plates.

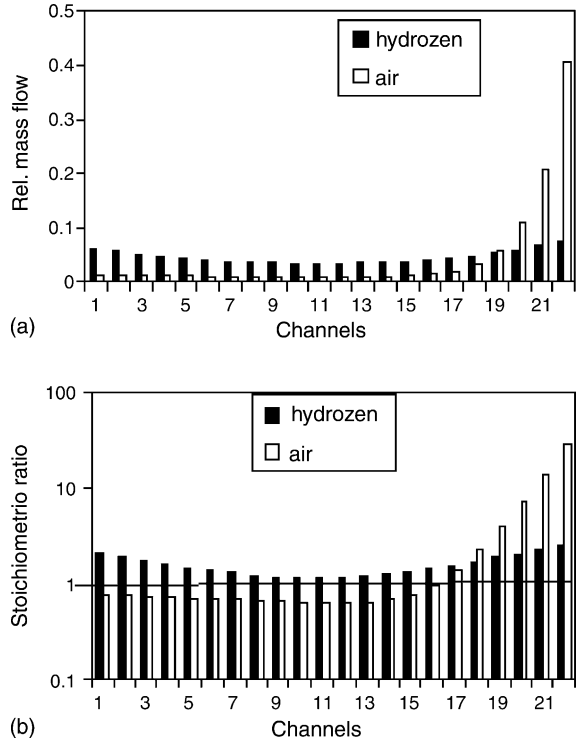

Fig. 9. (a) Relative flow distribution of hydrogen and air; (b) stoichiometric ratio of hydrogen and air in Z-type flow configuration.

5. Conclusions

The pressure loss in a fuel cell stack is one of the important determinates of overall fuel cell efficiency, while uniform flow distribution over the entire plate is necessary for optimum use of the entire active land area of the plate. Algorithms have been developed to calculate the plate pressure drop and flow distribution in multiple U- and Z-type flow configurations. These have been validated by comparing with results obtained from full three-dimensional CFD simulations.

Comparative assessment of different channel configurations shows that serpentine channels exhibit a significantly higher pressure drop while parallel configurations have a significantly high flow non-uniformity index. The latter can be reduced by using multiple-U type configurations without significant increase in pressure drop. Multiple Z-type configurations have, in general, a lower flow non-uniformity index but may have much higher pressure drop. There is also the possibility of mismatch between the flow distribution at the cathode side and the anode side and this results in off-design local stoichiometric ratios. Careful design of the flow configurations on distributor plates is therefore necessary to obtain optimum performance.

Acknowledgements

The CFD computations were performed using the facilities of the CFD Centre, IIT-Madras, India.

References

[1] S. Maharudrayya, S. Jayanti, A.P. Deshpande, J. Power Sources 144 (2005) 94–106.
[2] J.R. Kee, P. Korada, K. Walters, M. Pavol, J. Power Sources 109 (2002) 148–159.
[3] A. de Souza, E.R. Gonalez, J. Solid State Electrochem. 7 (2003) 651–657.
[4] S. Maharudrayya, S. Jayanti, A.P. Deshpande, J. Power Sources 138 (2004) 1–13.
[5] T.V. Ngyen, J. Electrochem. Soc. 143 (1996) 2767–2772.
[6] F. Barreras, A. Lozano, L. Valino, C. Marian, A. Pasau, J. Power Sources 144 (2005) 54–66.
[7] W.M. Kays, M.E. Crawford, Convective Heat and Mass Transfer, McGraw-Hill, New York, 1980.
[8] H. Dohle, R. Jung, N. Kimiaie, J. Muller, J. Power Sources 124 (2003) 371–384.
[9] G. Hu, J. Fan, S. Chen, Y. Liu, K. Cen, J. Power Sources 136 (2004) 1–9.
[10] K. Zkovesky, A. Pozio, J. Power Sources 130 (2004) 95–105.
[11] F.N. Büchi, S. Srinivasan, J. Electrochem. Soc. 144 (1997) 2767–2772.
[12] H.-M. Jung, W.-Y. Lee, J.-S. Park, C.-S. Kim, Int. J. Hydrogen Energy 29 (2004) 945–954.